



POLITECNICO MILANO 1863

Brief Analysis on SRM internal ballistics

AA 2023-2024

Space Propulsion course

Professor: Filippo Maggi

Person Code	Surname	Name
10713569	Grandinetti	Roberta
10765536	Mirri	Pietro
10730683	Nuccio	Gabriele

November 19, 2024

Contents

1	Introduction	4
2	Ballistic analysis	4
3	Monte Carlo approach	5
3.1	Convergence criterion	5
3.2	Population size	5
3.3	Monte Carlo results	5
4	Relative uncertainty analysis and conclusions	6
A	Appendix	8

Symbols List

a	Vieille's law parameter
n	Vieille's law parameter
σ	Uncertainty
\bar{x}	Mean value
c^*	Characteristic Velocity
t	t-student distribution factor
n_{mon}	Number of Monte Carlo simulations
t_b	Burning time
ν	Degrees of freedom
n_{pop}	Number of population variable
δ	Relative uncertainty

1 Introduction

The **BATES** (Ballistic Test and Evaluation System) kind rocket motor is a specific type of solid rocket motor widely used in research and testing of solid rocket propulsion and ballistics. The starting point of the reported analysis is a set of experimental data coming from 9 different batches of 27 nominally identical BATES motors, whose grain dimensions and composition features are showed hereafter:

Composition[1]			Dimensions	
Component	Mass percentage [%]	Density [kg m^{-3}]	Length [mm]	
Ammonium perchlorate	68	1950	Internal diameter [mm]	290
Aluminum	18	2700	External diameter [mm]	100
HTPB	14	920	Web thickness [mm]	160
				30

Table 1: Grain composition and geometrical features

Each propellant batch differ from each other just due to production variability and it's characterized by three pressure curves, respectively low, mid, high pressure, obtained changing the throat area of the nozzle accordingly with the pressure level.

Pressure level	Throat diameter [mm]
High	21.81
Medium	25.25
Low	28.8

Table 2: Throat diameter associated to each pressure level

Each trace refers to a single motor firing and reports the absolute pressure in bar with a sampling frequency of 1kHz.

2 Ballistic analysis

To perform the analysis on the SRM motors the Bayern Chemie (BC) method is adopted for each one of the aforementioned pressure curves. The first step is to identify the instants among which the SRM is considered active. This two points represent the instant of time when the pressure trace intercepts the 5% of the maximum pressure, instead of the usual 1% to increase the reliability of the performed analysis. To remove the effect of the ignition transient on the pressure trace the first twenty points were excluded from the following computations. After these two points are individuated the reference pressure is computed. One can then evaluate two other time instants where the pressure trace crosses the latter pressure value to compute the effective burning time of the engine from which the effective pressure and the burning rate are finally evaluated.

The analysis proceeds with the computation of the parameters a and n of the Vieille's law and their related mean values (a_{mean}, n_{mean}) and uncertainties (σ_a, σ_n), which provide the characterization of the whole propellant production (fitting over the full dataset). The results are summarized in the table 3 below:

Vielle's law parameter	Mean value	Uncertainty (σ)
a [$\text{mm}/(\text{s} \cdot \text{bar}^n)$]	1.7269	0.0184
n	0.3821	0.0027

Table 3: Ballistic data

Then, after computing the average density and consequently the total mass of propellant, from the definition of the c^* integrated over time, the experimental value of the c^* can be computed for each pressure curve, obtaining 27 different values hereafter graphically reported:

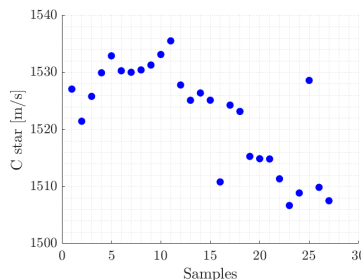


Fig. 1: c^* values for each trace

Under the assumption that c^* is changing only negligibly with respect to pressure, we can average the entire data set in order to obtain a mean $c_{mean}^* = 1523 \text{ ms}^{-1}$ and an uncertainty estimation $\sigma_{c^*} = 8.9603 \text{ ms}^{-1}$.

3 Monte Carlo approach

A Monte Carlo approach has been then adopted to perform uncertainties propagation and analysis [2]. Given the experimental nature of the ballistic data (3) their uncertainties are of aleatory type. At this stage random errors are usually assumed to come from a Gaussian distribution, but since the number of samples is limited in this case, in particular less than 30, a t-student distribution at a degree of freedom $\nu = n_{samples} - 1 = 26$ appears as a more appropriate choice. After that, the populations of a, n and c^* are propagated according to the following law: $x_{pop} = \bar{x} + t \cdot \sigma_x$

where x are the variables for which the populations are computed. t is a random generated number considering a t-student distribution with the Matlab function *trnd.m*.

3.1 Convergence criterion

In order to determine whether the results of the simulation are stable and accurate enough is necessary to establish satisfactory convergence criteria. A relative error-based criterion is applied to the mean values of a single Monte Carlo simulation, which will be further explained later as the population size has to be determined first.

After achieving the convergence of a single Monte Carlo analysis, it is necessary to ensure its repeatability. For different populations, the values obtained could slightly differ within the interval described by the standard deviation, requiring some refinement. To achieve this, multiple Monte Carlo simulations must be run, ultimately obtaining the mean of the burning times with the required precision. The precision threshold value was selected as the typical minimum accuracy sought for burning rate measurements in solid rocket engine design (1% [4]). The laws to determine the number of Monte Carlo simulations needed (n_{mon}) are [3]:

$$\bar{\sigma}_{t,burn} = \frac{\sigma_{t,burn}}{\sqrt{n_{mon}}} \quad \frac{3\bar{\sigma}_{t,burn}}{\bar{t}_{burn}} = 0.01$$

The interval of $3\bar{\sigma}$ is necessary to have a confidence of 99.73% over the obtained precision. After multiple analysis a conservative estimation is obtained as $n_{mon} = 85$.

3.2 Population size

Choosing an appropriate population size is crucial for balancing accuracy and computational efficiency. The population size has not been chosen a priori, but through an iterative process, in which at every step every population number was tested several times in order to statistically check the reliability of convergence. The goal was computing the population number that would provide a successful convergence 100 consecutive times (probability of success over 99%), based on the relative error criterion at the end of the Monte Carlo simulation. The chosen threshold guarantees the convergence within the value of 10^{-5} for each Monte Carlo run.

$$\frac{|\bar{t}_{burn,(end-1)} - \bar{t}_{burn,end}|}{\bar{t}_{burn,end}} \cdot 100\% \leq 0.001\%$$

Eventually a number of populations $n_{pop} = 20$ has been detected as the smallest size able to provide results compatible with the established convergence criterion with the required probability.

3.3 Monte Carlo results

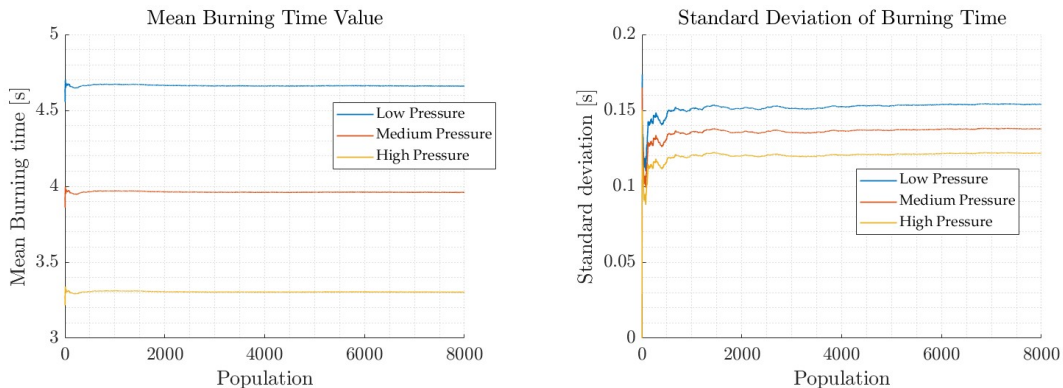


Fig. 2: Mean burning time and Standard deviation vs total population

Here are presented the results for all the pressure traces. As expected the mean burning time and the respective standard deviation are smaller for higher estimated pressure. Both the mean and the standard deviation satisfy the convergence requirements.

A targeted analysis is then performed only on the medium pressure trace, characterized by multiple Monte Carlo simulations. The burning time obtained for $n_{mon} = 85$ is $t_b = 3.947$ s, with a standard deviation of the Monte Carlo simulation of $\bar{\sigma} = 0.0206$ s, which guarantees the prediction reliability of the result. The latter is the standard deviation of the burning time means, not of the burning time itself, which decrease more slightly with respect to the single simulation value $\sigma = 0.0939$ s. Graphs of the evolution of t_b during the 85 Monte Carlo runs are shown in the Appendix A.

4 Relative uncertainty analysis and conclusions

The relative uncertainty for a and n in a Monte Carlo simulation depends on the chosen population size and is computed as $\delta = \frac{\sigma}{\bar{x}}$. Notably, when the population is small, the discrepancy with the experimental result may be significant, since it depends on the randomly generated population. Therefore, the standard deviation and the mean could be randomly higher or lower. However, as the population size increases, they gradually align with the standard deviation used to create them, according to a phenomenon attributed to the Law of Large Numbers [5]. Furthermore the single variable population (n_{pop} , the population of the generated a , n and c^*) is generated as previously said considering a Student t-distribution. This, for a degree of freedom of $\nu = n_{test} - 1 = 26$, leads to an increase in the standard deviation of [7]:

$$\frac{\sigma_t - \sigma_n}{\sigma_n} \cdot 100\% = \left(\frac{\sqrt{\frac{\nu}{\nu-2}} - 1}{1} \right) \cdot 100\% = 3.92\%$$

Moreover, an in-depth analysis can be conducted on the results obtained from Monte Carlo simulation. To calculate the standard deviation, the following formula holds: $\sigma = \sqrt{\frac{1}{n_{pop}-1} \sum_{i=1}^{n_{pop}} (x_i - \bar{x})^2}$. The $n_{pop} - 1$ term at the denominator is known as the Bessel's correction factor. It is necessary when the sample size is small, as it adjusts for the tendency to underestimate the population standard deviation. [6].

However, considering the total population of 8000 data points (n_{pop}^3) in our analysis, the overall relative uncertainty is lower than that obtained from the initial 20 data points generated. In the first place the mean of the single variable population and the overall Monte Carlo one is the same. However since each data point in its population is considered is considered 400 times (n_{pop}^2), the formulas for the computation of standard deviations of the initial population and the overall population differ from each other:

$$\begin{aligned} \sigma_{overall} &= \sqrt{\frac{n_{pop}^2}{n_{pop}^3 - 1} \sum_{i=1}^{n_{pop}} (x_i - \bar{x})^2} = \sqrt{\frac{400}{7999} \sum_{i=1}^{20} (x_i - \bar{x})^2} \\ \sigma_{single} &= \sqrt{\frac{1}{n_{pop} - 1} \sum_{i=1}^{n_{pop}} (x_i - \bar{x})^2} = \sqrt{\frac{1}{19} \sum_{i=1}^{20} (x_i - \bar{x})^2} \end{aligned}$$

As the population grows, the multiplicative term tends towards $\sqrt{1/n}$, inherently neglecting the Bessel's correction factor, as a larger population becomes more representative of all possible cases. In our analysis, for a single-variable population of 20 and a total population of 8000, the ratio between the standard deviations is $\text{Ratio}_\sigma = \frac{\sigma_{overall}}{\sigma_{single}} \approx 0.975$

Therefore, the relative uncertainty of this Monte Carlo analysis is decreasing by around 2.5% with respect to the one of the single variable population, while with respect to the test uncertainties the ratio vary for every randomly generated population. To conclude, considering the relative uncertainties after the 85 Monte Carlo simulations, the relative uncertainties are:

$$\delta_{a,mc} = \frac{\sigma_a}{a_{mean}} = 0.0109 \qquad \delta_{n,mc} = \frac{\sigma_n}{n_{mean}} = 0.0071$$

These results further demonstrate the effectiveness of multiple Monte Carlo simulations. The relative uncertainties are very similar to those obtained from the test $\delta_{a,test} = 0.0107$ and $\delta_{n,test} = 0.0072$.

References

- [1] F. Maggi. Space Propulsion Course Notes.
- [2] Joint Committee for Guides in Metrology. Evaluation of measurement data — an introduction to the ‘guide to the expression of uncertainty in measurement - propagation of distributions using a monte carlo method.
- [3] Sergio Ricci Gian Luca Ghiringhelli, Giuseppe Gibertini. *Dispense di fondamenti di sperimentazione aerospaziale*. 2022.
- [4] Adriano Annovazzi Luigi T. DeLuca. Survey of burning rate measurements in small solid rocket motors. <https://www.sciencedirect.com/science/article/pii/S2667134423000573>.
- [5] Pál Révész. *The Laws of Large Numbers*. ACADEMIC PRESS INC., 1968.
- [6] Russell T. Warne. *Statistics For The Social Sciences: A General Linear Model Approach*. Cambridge University Press, 2017.
- [7] Brian Gerard Williams. *Biostatistics: Concepts and Applications for Biologists*. CHAPMAN HALL, 1993.

A Appendix

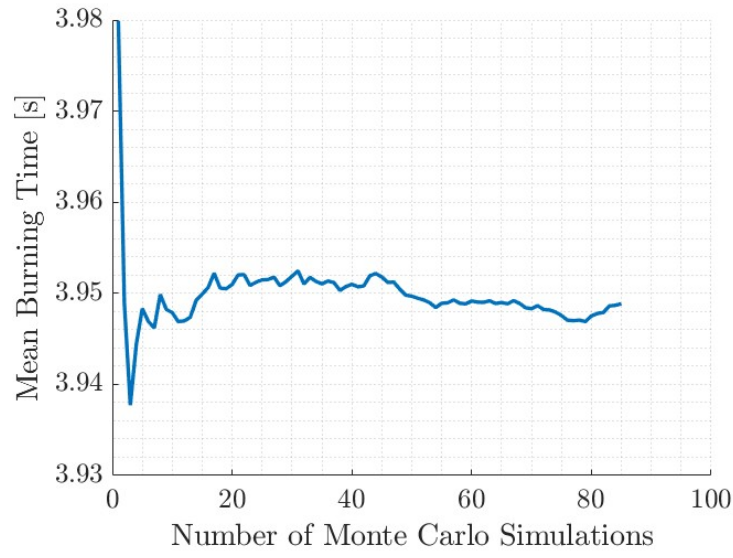


Fig. 3: Mean Value of the burning time vs number of Monte Carlo method simulations

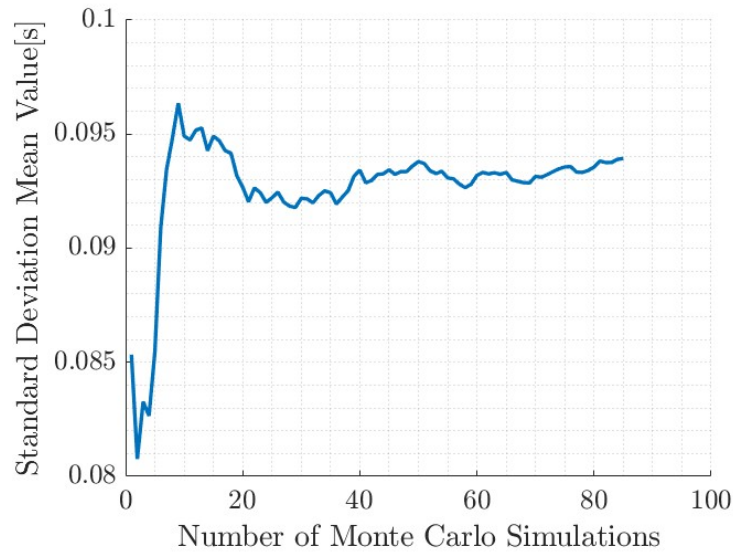


Fig. 4: Standard Deviation of the burning time vs number of Monte Carlo method simulations